Journal of Power and Energy Engineering, 2025, 13(1), 1-17
https://www.scirp.org/journal/jpee
ISSN Online: 2327-5901
ISSN Print: 2327-588X

Real-Time Error Analysis of Multi-Channel Capacitive Voltage Transformer Using Co-Prediction Matrix

Jiusong Hu[1], Ao Xiong[1], Yongqi Liu[2], Guaxuan Xiao[3], Yi Zhong[4]

[1]College of Railway Transportation, Hunan University of Technology, Zhuzhou, China
[2]Wasion Group Co., Ltd., Changsha, China
[3]State Grid Zhejiang Leqing Power Supply Co., Ltd., Leqin, China
[4]Shengtong Electric New Energy Technology Co., Ltd., Jurong, China
Email: xiongao991225@163.com, www.liubin629.net@163.com, 28732654@qq.com

How to cite this paper: Hu, J.S., Xiong, A., Liu, Y.Q., Xiao, G.X. and Zhong, Y. (2025) Real-Time Error Analysis of Multi-Channel Capacitive Voltage Transformer Using Co-Prediction Matrix. *Journal of Power and Energy Engineering*, **13**, 1-17.
https://doi.org/10.4236/jpee.2025.131001

Received: December 29, 2024
Accepted: January 21, 2025
Published: January 24, 2025

Abstract

Capacitive voltage transformers (CVTs) are essential in high-voltage systems. An accurate error assessment is crucial for precise energy metering. However, tracking real-time quantitative changes in capacitive voltage transformer errors, particularly minor variations in multi-channel setups, remains challenging. This paper proposes a method for online error tracking of multi-channel capacitive voltage transformers using a Co-Prediction Matrix. The approach leverages the strong correlation between in-phase channels, particularly the invariance of the signal proportions among them. By establishing a co-prediction matrix based on these proportional relationships, The influence of voltage changes on the primary measurements is mitigated. Analyzing the relationships between the co-prediction matrices over time allows for inferring true measurement errors. Experimental validation with real-world data confirms the effectiveness of the method, demonstrating its capability to continuously track capacitive voltage transformer measurement errors online with precision over extended durations.

Keywords

Capacitive Voltage Transformers, Co-Prediction Matrix, High-Voltage, Measurement error

1. Introduction

Electric power transformers are indispensable in power networks, where they perform voltage stepping down and stepping up to ensure the efficient transmission

and distribution of electrical energy. Accurate measurement and monitoring of transformation errors are critical for maintaining grid operational integrity, ensuring reliable trade settlements and relay protection functions, and supporting advanced applications within smart grids [1] [2]. Continuous monitoring of these errors can also provide early warnings of potential issues such as insulation degradation or winding deformation, thus preventing outages caused by transformer failures [3] [4]. The development of smart grids has introduced new sensing and data transmission technologies like electronic transformers and digital merging units, which, while offering many advantages over traditional current transformers (CTs) and voltage transformers (PTs), present more unstable measurement errors and complex variation patterns. Therefore, tracking the operational errors of these new types of transformers has become particularly important, presenting a significant challenge for experts in the measurement field [5].

At present, the verification of transformers mainly relies on "static verification". This method requires power interruption, which makes the process time-consuming, and the high-precision reference standard equipment used is bulky and difficult to carry [6]-[8]. In order to improve efficiency and overcome these limitations, research work focuses on the integration, standardization, and automation of static verification. With the advancement of technology, "online verification" as a new method has gradually become possible. It can detect errors without power outages, thereby significantly reducing the impact on the daily operation of the power grid. In view of this, it is particularly important to develop real-time monitoring methods suitable for non-power outage conditions [9].

References [10] and [11] proposed abnormal monitoring methods based on physical or mathematical models, but these methods have strong model dependence and sensor dependence and face limitations in engineering applications. Reference [12] uses signal processing technology to solve the problem of detecting error changes of the order of 0.1%. However, due to the large primary voltage fluctuations caused by factors such as grid load changes and active voltage regulation, this method is difficult to effectively distinguish normal fluctuations from abnormal fluctuations, and is prone to misjudgment, affecting the recognition accuracy.

On the other hand, reference [13] proposes a method based on independent component analysis (ICA), whereas reference [14] is based on principal component analysis (PCA). Both methods regard the three-phase CVT at the same measurement point as an evaluation group and obtain real-time statistical data reflecting the error state by separating and reconstructing the secondary output signals. However, these methods do not perform well in the face of actual environmental conditions such as significant three-phase voltage imbalance.

To address these challenges, this paper proposes a new method for online error tracking of multi-channel CVTs based on a co-prediction matrix. First, the strong correlation between in-phase channels, especially the signal ratio invariance between these channels, is used to construct a co-prediction matrix to

mitigate the impact of primary voltage measurement fluctuations. Subsequently, the true measurement error is inferred by analyzing the relationship of the co-prediction matrix over time. The effectiveness of the proposed method is experimentally verified using real data collected from a 330 kV substation in Northwest China, demonstrating that the method is capable of online and continuous tracking of CVT measurement errors with an accuracy of 0.01% over a long period of time.

2. Preliminaries

2.1. CVTs Measurement Principle

CVT is a special transformer used to convert high-voltage primary measurement signals into low-voltage secondary outputs suitable for measurement. Its structure, shown in Figure 1, consists of two parts: a capacitive voltage divider and an intermediate transformer. The capacitive voltage divider achieves a voltage reduction through capacitive division to obtain a low-voltage output suitable for measurement. In this setup, the division capacitors C_M and C_H are connected in series, and different voltage division ratios can be obtained by adjusting their sizes. Figure 1, U_p represents the primary input voltage, U_s represents the secondary output voltage measurement, L denotes the compensating inductor, and D denotes residual windings. The intermediate transformer further reduces the low voltage signal from the capacitive divider to a suitable range for measurement, protection, and communication CVTs are manufactured by different manufacturers, and their parts can be affected by the surrounding conditions. This leads to differences between the voltage they actually produce and what they should ideally produce, which is referred to as a measurement error. Official rules state that these errors can affect how well the voltage matches in terms (ratio errors) or timing (phase errors). The primary focus is on the first type: the proximity of the actual voltage level to the expected value. In voltage measurement,

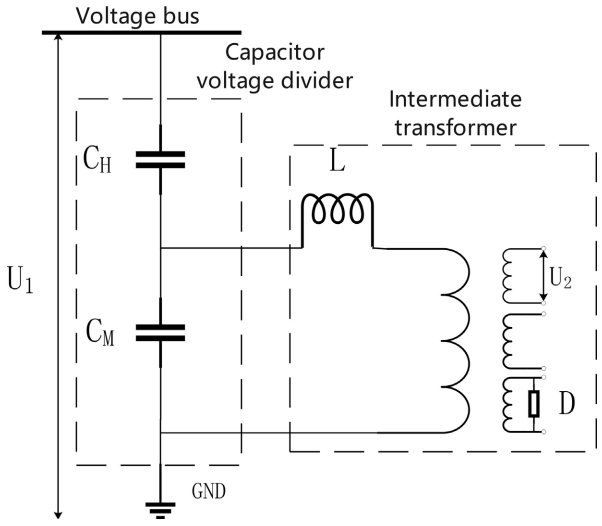

Figure 1. CVT structure diagram.

this discrepancy is referred to as the "ratio difference," which can be described using an equation, as shown in Equation (1).

Table 1. CVT accuracy classes and corresponding ratio errors.

Accuracy class	Ratio Error $\varepsilon(\pm\%)$
0.2	0.2
0.5	0.5
1.0	1.0
3.0	3.0
3P	3.0
6P	6.0

$$\varepsilon(t)=\frac{k_r U_s(t)-U_p(t)}{U_p(t)}\times 100\% \tag{1}$$

where $\varepsilon(t)$ represents the ratio error of the CVT at time t, k_r is the nominal transformation ratio of the CVT; and $U_p(t)$ and $U_s(t)$ represent the primary and secondary voltages of the CVT at time t, respectively.

The measurement error level of CVT can be described by its accuracy class. According to national standards, within the specified range of primary voltage and secondary load variations, when the load power factor is at its rated value, the maximum value of the voltage error represents the accuracy class. This is typically expressed as a percentage, such as 0.2, 0.5, 1, 3, etc., as shown in Table 1.

2.2. Analysis of Primary Side Input Characteristics of CVT

The operation mode of the power system and the electrical connection relationship between CVTs impose restrictions on the layout of CVTs, exhibiting the characteristics of symmetrical distribution and electrical correlation. In high-voltage substations, the configuration of CVTs is affected by the primary wiring method. Typically, multiple groups of CVTs are used to measure the voltage on the same bus to ensure accuracy. In double-bus or double-bus segmented wiring and 3/2 wiring, the primary side of all the CVTs is connected to the same bus; therefore, the input voltage is equal.

$$U_{p1}(t)=U_{p2}(t)=\cdots=U_{pn}(t) \tag{2}$$

where $U_p(t)$ represents the amplitude of the busbar voltage and $U_{pn}(t)$ represents the amplitude of the primary measurement voltage of CVT-n.

2.3. Analysis of Secondary Side Output Characteristics of CVT

CVTs are a special type of transformer that converts high-voltage signals from the busbar into low-voltage signals. According to Equation (3), the secondary output of the CVT can be derived as follows.

$$\begin{aligned} U_s &= U_s + \Delta U \\ &= \begin{pmatrix} \frac{1+\varepsilon_1(t)}{k_r} & 0 & \cdots & 0 \\ 0 & \frac{1+\varepsilon_2(t)}{k_r} & \cdots & 0 \\ \vdots & \vdots & \ddots & \vdots \\ 0 & 0 & \cdots & \frac{1+\varepsilon_n(t)}{k_r} \end{pmatrix} \times \begin{pmatrix} U_{p1}(t) \\ U_{p2}(t) \\ \vdots \\ U_{pn}(t) \end{pmatrix} \pm \begin{pmatrix} \Delta U_1(t) \\ \Delta U_2(t) \\ \vdots \\ \Delta U_n(t) \end{pmatrix} \end{aligned} \tag{3}$$

where $\varepsilon_n(t)$ represents the ratio error of the nth CVT at time t, $U_{sn}(t)$ and $U_{pn}(t)$ represent the primary and secondary voltages of the nth CVT at time t respectively, and $\Delta U_n(t)$ represents the magnitude of the voltage fluctuations caused by the three-phase load asymmetry.

Owing to the absence of load asymmetry in the correlation relationship, $\Delta U_n(t)$ is 0 in Equation (3), which is simplified to Equation (4).

$$\begin{pmatrix} U_{s1}(t) \\ U_{s2}(t) \\ \vdots \\ U_{sn}(t) \end{pmatrix} = \begin{pmatrix} \frac{1+\varepsilon_1(t)}{k_r} & 0 & \cdots & 0 \\ 0 & \frac{1+\varepsilon_2(t)}{k_r} & \cdots & 0 \\ \vdots & \vdots & \ddots & \vdots \\ 0 & 0 & \cdots & \frac{1+\varepsilon_n(t)}{k_r} \end{pmatrix} \times \begin{pmatrix} U_{p1}(t) \\ U_{p2}(t) \\ \vdots \\ U_{pn}(t) \end{pmatrix} \tag{4}$$

According to the research in Section B regarding the connection methods of CVTs, the primary-side input voltage of the same-phase CVTs on the same bus is equal. Therefore, the secondary voltage amplitudes of single-phase CVTs operating at the same voltage level exhibit the following relationship.

$$\frac{u_{s1}(t)}{u_{sn}(t)} = \frac{1+\varepsilon_1(t)}{1+\varepsilon_n(t)} \tag{5}$$

$u_{s1}(t)$ and $u_{sn}(t)$ represent the initial and subsequent secondary-side output voltages, respectively. $\varepsilon_1(t)$ is defined as the first ratio error at time t, and correspondingly, $\varepsilon_n(t)$ represents the n-th ratio error at the same time t.

3. Methodology

In this section, a detailed explanation of the algorithmic principles, derivation, and process of the proposed method is presented.

3.1. Error Tracking

CVTs with at least three channels of the same phase were examined. Based on Equations (4) and (5), which represent the invariance of the ratio relationship between same-phase channels, the co-proportional matrix $X(t) \in \mathbb{R}^{n\times n}$ at sampling point t is defined as shown in Equation (6). This matrix captures the ratio relationships between the measurement errors of all the channels in the CVTs at

time t.

$$X(t)=\begin{pmatrix}u_{s1}(t)\\ \vdots \\ u_{sn}(t)\end{pmatrix}\times\begin{pmatrix}u_{s1}^{-1}(t)\\ \vdots \\ u_{sn}^{-1}(t)\end{pmatrix}^{\mathrm{T}}=\begin{pmatrix}1 & \cdots & \dfrac{u_{s1}(t)}{u_{sn}(t)}\\ \vdots & \ddots & \vdots \\ \dfrac{u_{sn}(t)}{u_{s1}(t)} & \cdots & 1\end{pmatrix}$$
$$=\begin{pmatrix}1 & \cdots & \dfrac{1+\varepsilon_1(t)}{1+\varepsilon_n(t)}\\ \vdots & \ddots & \vdots \\ \dfrac{1+\varepsilon_n(t)}{1+\varepsilon_1(t)} & \cdots & 1\end{pmatrix} \tag{6}$$

When a CVT undergoes error variation at time t, the co-proportional matrix $X(t)$ exhibits significant fluctuations compared to $X(t-1)$. Therefore, matrix $H(t)\in\mathbb{R}^{i\times j}$ is defined to represent the relationship between the co-proportional matrices at times t and $t-1$, and its elements are calculated according to Equation (7).

$$H_{i,j}(t)=\frac{X_{i,j}(t-1)}{X_{i,j}(t)}=\frac{1+\varepsilon_i(t-1)}{1+\varepsilon_j(t-1)}\cdot\frac{1+\varepsilon_j(t)}{1+\varepsilon_i(t)} \tag{7}$$

In the equation, $H_{i,j}(t)$ and $X_{i,j}(t)$ represent the elements in the ith row and jth column of matrices $H(t)$ and $X(t)$ at time t. Additionally, $X_{i,j}(t)$ represents the ratio of the secondary voltage measurements between CVT-i and CVT-j. Furthermore, $H_{i,j}(t)$ is calculated based on the amplitude of the secondary output voltage.

Combining Equation (6), matrix $H(t)$ can be represented as Equation (8).

$$H(t)=\begin{pmatrix}1 & \cdots & \dfrac{1+\varepsilon_1(t-1)}{1+\varepsilon_j(t-1)}\cdot\dfrac{1+\varepsilon_i(t)}{1+\varepsilon_1(t)}\\ \vdots & \ddots & \vdots \\ \dfrac{1+\varepsilon_i(t-1)}{1+\varepsilon_1(t-1)}\cdot\dfrac{1+\varepsilon_1(t)}{1+\varepsilon_j(t)} & \cdots & 1\end{pmatrix} \tag{8}$$

According to Equation (7), the measurement error ε_j of the jth CVT at time t can be derived using the calculation detailed in Equation (9).

$$\varepsilon_j(t)=\left(1+\varepsilon_j(t-1)\right)\cdot\frac{1+\varepsilon_i(t)}{1+\varepsilon_i(t-1)}\cdot H_{i,j}(t)-1 \tag{9}$$

At time t, in Equation (9), CVT-i and CVT-j at time $t-1$ are known values. If this is the first evaluation point of the sample, it represents the initial error of CVT.

When there is no change in the measurement error at times t and $t-1$, that is, $\varepsilon_i(t)=\varepsilon_i(t-1)$, the magnitude of the measurement error of CVT-j is denoted as $\varepsilon_j(t)\big|_i$, as shown in Equation (10).

$$\varepsilon_j(t)\big|_i=\left(1+\varepsilon_j(t-1)\right)\cdot H_{i,j}(t)-1 \tag{10}$$

where $\varepsilon_j(t)\big|_i$ represents the measurement error of the jth CVT when the ith CVT remains constant.

By combining Equation (8) and Equation (10), a matrix composed of errors can be obtained, referred to as the co-prediction matrix $\varepsilon^{\text{pre}}(t) \in \mathbb{R}^{i\times j}$, where ε^{pre} represents the predicted error. This is detailed in Equation (11).

$$\varepsilon^{\text{pre}}(t) = \begin{pmatrix} \varepsilon_1^{\text{pre}}(t) \\ \varepsilon_2^{\text{pre}}(t) \\ \vdots \\ \varepsilon_i^{\text{pre}}(t) \end{pmatrix} = \begin{pmatrix} \varepsilon_1(t-1)\big|_1 & \varepsilon_2(t)\big|_1 & \cdots & \varepsilon_j(t)\big|_1 \\ \varepsilon_1(t)\big|_2 & \varepsilon_2(t-1)\big|_2 & \cdots & \varepsilon_j(t)\big|_2 \\ \vdots & \vdots & \ddots & \vdots \\ \varepsilon_1(t)\big|_i & \varepsilon_2(t)\big|_i & \cdots & \varepsilon_j(t-1)\big|_i \end{pmatrix} \tag{11}$$

The physical meaning of this equation is as follows: at time t, compared with time t-1, if the i-th CVT does not experience an error drift, it indicates the measurement error magnitude of the other CVTs. $\varepsilon_i^{\text{pre}}(t)$ represents the measurement error row vector at time t in the i-th row. The establishment of the co-prediction matrix enables quantitative calculation and real-time tracking of the monitored CVT measurement errors.

3.2. Error Change Positioning

In the co-prediction matrix, the elements related to the CVT with error changes correspondingly change, whereas those unaffected will remain relatively stable. Based on this characteristic, these changes can be identified by comparing the predicted error values over the time series, and an error localization matrix $\Delta\varepsilon(t)$ can be defined. The Specific Calculation Methods for this matrix are shown in Equation (12).

$$\Delta\varepsilon(t) = \begin{pmatrix} \varepsilon_1^{\text{pre}}(t) \\ \varepsilon_2^{\text{pre}}(t) \\ \vdots \\ \varepsilon_i^{\text{pre}}(t) \end{pmatrix} - \begin{pmatrix} \varepsilon^{ret} \\ \varepsilon^{ret} \\ \vdots \\ \varepsilon^{ret} \end{pmatrix} \tag{12}$$

where ε^{ret} represents the newly updated error vector.

Owing to the random fluctuations present in CVTs, even if they are co-related, the elements in the co-proportion matrix may not be exactly equal over the time series when no error changes occur in the CVTs. However, they may exhibit only minor fluctuations. These fluctuations can be filtered by setting a threshold, calculated using Equation (13).

$$-\alpha < \Delta\varepsilon_{i,j}(t) < \alpha, (i \neq j) \tag{13}$$

where $\Delta\varepsilon_{i,j}(t)$ and $\alpha \in [-0.0001, 0.0001]$ represent the error in the i-th row and j-th column of $\Delta\varepsilon(t)$ and the set threshold, respectively.

In the event of a power outage, if the system deviation prior to the outage remains within the accuracy standard of 0.2, the latest error vector of the system post-restoration can be estimated by averaging the most recent 100 error vectors ε^{ret}. This approach ensures data continuity and maintains system stability.

4. Algorithm Process

The algorithm process for the online error tracking of CVTs based on the co-prediction matrix is illustrated in Figure 2. The process of this method is summarized as follows.

1) Data Collection: The online monitor uses CVT error characteristics to collect high-precision information from the secondary output data of CVTs that are newly installed in the substation or have recently undergone periodic testing. These data were used to establish an initial sampling dataset and real-time evaluation dataset.

2) Initialization Phase: During initialization, the initial sampling dataset is used to set up the co-proportional matrix for the CVTs. At time $t = 0$, this matrix is denoted as X_0, Which forms the basis for subsequent error evaluations.

3) Construction and Updating during Online Monitoring: In online monitoring phase, the co-proportion matrix $X(t)$ is constructed for the current time *t*. This matrix was then combined with the previous co-proportion matrix $X(t-1)$ from time $t-1$ to calculate the co-prediction matrix $\varepsilon^{\text{pre}}(t)$. Subsequently, $X(t-1)$ is updated to $X(t)$ for the current time t, preparation for the next iteration.

4) Error Assessment and Localization during Online Monitoring: During error assessment and localization phase, error tracking is performed by comparing the difference between the co-prediction matrix $\varepsilon^{\text{pre}}(t)$ and the latest returned error vector ε^{ret}. At $t = 1$, ε^{ret} was initialized to zero. If the difference falls within the predefined accuracy level error limit α, the error vector ε^{ret} is updated. The error state is then quantified based on the latest ε^{ret}, and the next round of evaluation is initiated.

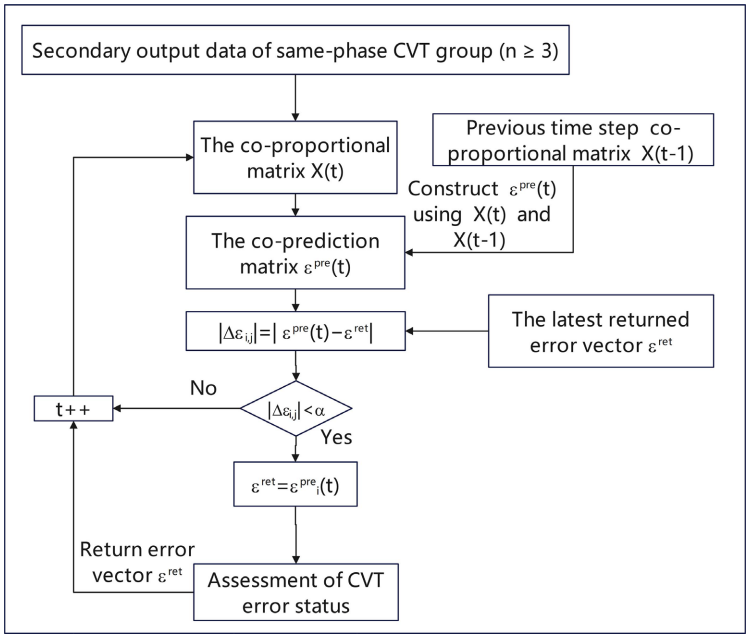

Figure 2. Online error tracking method algorithm.

5. Experiment and Results

The effectiveness of the CVT online tracking method was validated using a co-prediction matrix. Secondary output voltage signals from the online operation of qualified CVTs were collected to construct an error-free online dataset and an online monitoring dataset with various errors. The accuracy and effectiveness of the method were verified by comparing the monitoring dataset with the added errors against the measurement errors of the method.

5.1. Experimental Environment

The experiment was conducted on CVTs operating in a 330 kV substation in Northwest China, which employs a 3/2 wiring configuration where outgoing lines are connected to CVTs labeled A, B, and C. All CVTs, model TYD300/3-0.005 with an accuracy class of 0.2, were manufactured by Xi'an Xirong Electric Power Capacitor Co., Ltd. To ensure experimental accuracy, the initial errors of all the CVTs were set to zero. To precisely capture the secondary voltage signals, a high-precision acquisition device with an accuracy level of 0.01 was selected (see Figure 3 and schematic in Figure 4). This device features a 24-bit A/D converter at the sampling rate of 10 kHz and outputs data every three minutes. According to the acceptance test for substation, the ratio errors of three CVTs of the A phase are recorded from the test reports, as shown in Table 2.

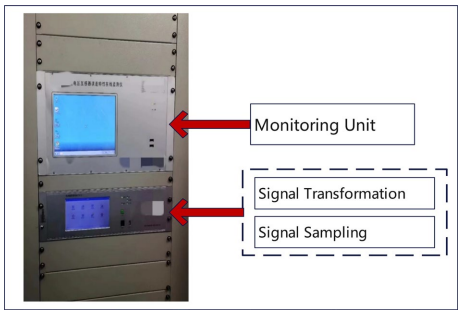

Figure 3. On-site installation of the sampling device.

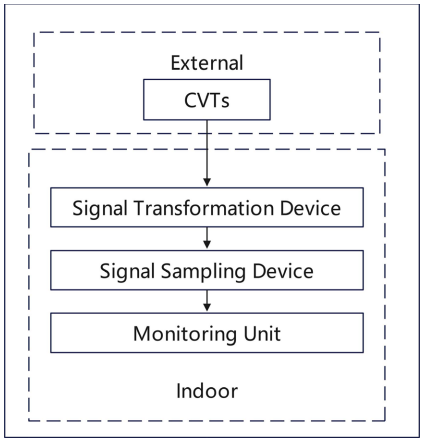

Figure 4. Monitoring system.

Over a continuous period of 15 days, comprehensive data acquisition was conducted on nine CVTs, with each CVT collecting 7200 data points. To verify the high accuracy and reliability of the collected data, the measured voltages (U_s) were converted to primary side voltages (U_p) using the nominal transformation ratio, and the ratio errors of the three CVTs were calculated using Equation (1). The ratio error curves and voltage waveforms are shown in Fig.5. By comparing the ratio error curves in Figure 5 with the numerical values listed in Table 2, it was observed that the ratio errors of the CVTs showed no significant deviation from the acceptance test results and complied with the 0.2 level precision requirement specified in Table 1.

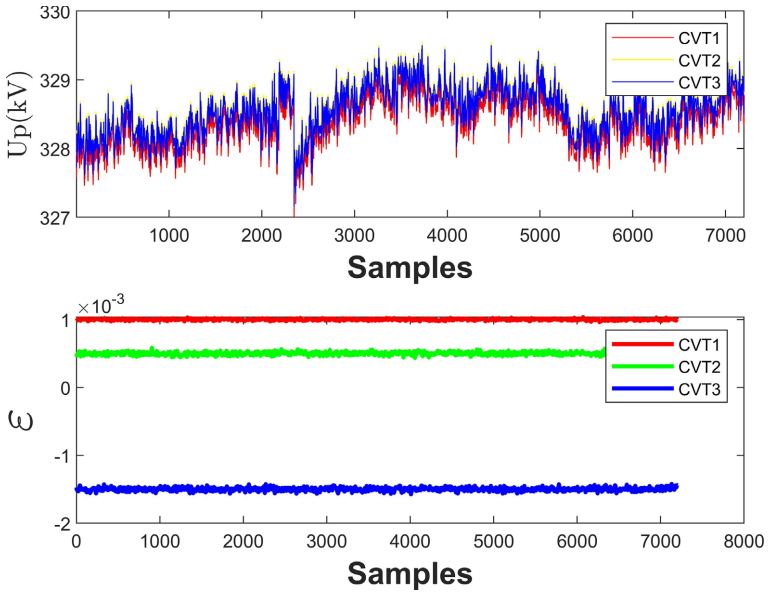

Figure 5. The amplitudes and ratio errors of A-Phase CVTs.

Table 2. Ratio errors of each a-phase CVT during acceptance testing.

CVTNum-A	Ratio error
CVT1-A	0.001
CVT2-A	0.0005
CVT3-A	−0.0015

5.2. Experimental Steps

1) Based on the basic conditions and data collection of the substation, the initial dataset was constructed from the first one thousand sampling points of three phase a CVTs, $X_i^{in} = \left[x_1^{in}, x_2^{in}, x_3^{in}\right] \in \mathbb{R}^{1000\times 3}$. Subsequently, sampling points 1001 to 7200 were designated as the monitoring dataset without added set error, $X_i^{Ev} = \left[x_1^{Ev}, x_2^{Ev}, x_3^{Ev}\right] \in \mathbb{R}^{6200\times 3}$.

2) Different true error datasets were constructed for the CVTs with varying settings across different periods, denoted as $\varepsilon^{Tru} = \left[\varepsilon_1^{Tru}, \varepsilon_2^{Tru}, \cdots, \varepsilon_{5200}^{Tru}\right]$. This

dataset was added to the last 5200 data points of the monitoring dataset $X_i^{Ev} = \left[x_1^{Ev}, x_2^{Ev}, x_3^{Ev}\right] \in \mathbb{R}^{6200\times3}$ for CVT1, whereas the other two groups of CVTs remained unchanged. After processing, the first set of experimental data was obtained as $X_i^{Ev} = \left[x_1^{Ev} \times \left(1+\varepsilon^{Tru}\right), x_2^{Ev}, x_3^{Ev}\right] \in \mathbb{R}^{6200\times3}$, from which the measurement error value and its variation for the CVT were calculated.

3) Step 2 was repeated for the remaining two CVTs. The predicted error value and variations in the predicted errors for the CVT were recorded separately for subsequent analysis and discussion.

5.3. Accuracy Results

In the experiment, we conducted a detailed analysis of the predicted error values, with the key metric being the predicted bias ε^{bia}, which is defined as the difference between the predicted error value ε^{pre} obtained through the co-prediction matrix and the true error value ε^{tru}. The calculation formula is $\varepsilon^{\text{bia}} = \varepsilon^{\text{pre}} - \varepsilon^{\text{tru}}$. To evaluate the performance under different conditions, various magnitudes of true errors were introduced into the CVT monitoring dataset at different times (see Table 3): for CVT1, with errors of 0.002, 0.0016, and 0.0015 for CVT2 and CVT3, errors of 0.001 and 0.0012 were set, respectively. Fig.6 shows the changes in each CVT over time or sample sequence, with the x-axis representing the time or sample number and the y-axis representing the predicted error value ε^{pre}.

As shown in Figure 6, CVT1 did not have a true error added in the sample interval from 0 to 1000, resulting in a predicted error that is essentially zero. In the sample interval from 1000 to 2500, the predicted error aligns well with the set true error of 0.002. Subsequently, in the sample interval from 2500 to 4000, the predicted error is approximately 0.0015, which was consistent with the added true error. Finally, in the sample interval from 4000 to 6200, the predicted error remained at approximately 0.0016, which matched the set true error. Similar error tracking results were obtained for CVT2 and CVT3, where the predicted errors at different sample intervals matched the set true errors. These results clearly demonstrate the effectiveness of using a co-prediction matrix for error tracking.

Table 3. True error settings for CVTs.

CVTNum-A	Sample segment	ε^{Tru}
CVT1	1000 - 2500	0.0020
CVT1	2500 - 4000	0.0015
CVT1	4000 - 6200	0.0016
CVT2	2000 - 6200	0.0010
CVT3	3000 - 6200	0.0012

Combining the data from Table 4 and Figure 7 further illustrates the maximum absolute predicted bias values for each CVT. CVT1 performed exceptionally well,

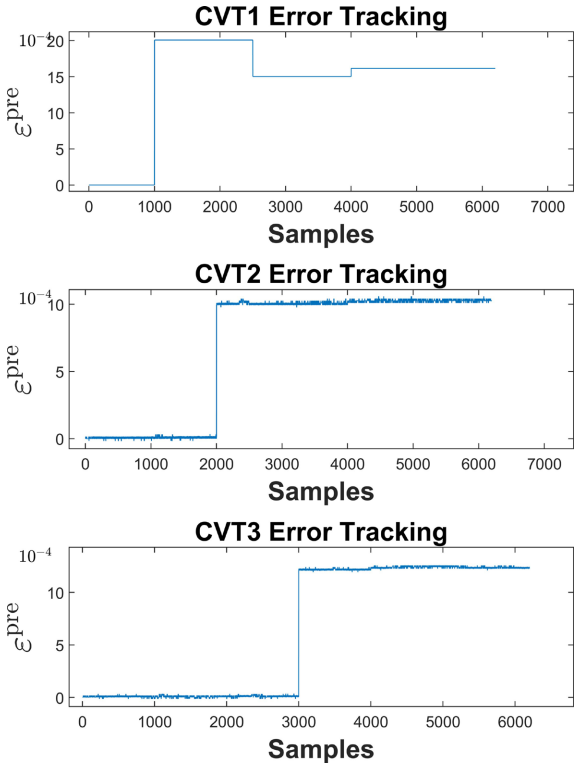

Figure 6. Predicted error tracking curves for each CVT a phase.

with a maximum predicted bias of only 0.0016%, whereas the maximum predicted biases for the other two CVTs were controlled within 0.0037%. Overall, the measurement error accuracy obtained by this method is less than 0.01%, which is significantly better than the requirements of the traditional 0.5-class transformer calibration standard. This demonstrates that the proposed method is not only effective but also highly practical, showing significant potential for improving the monitoring accuracy of Capacitive Voltage Transformers in power systems.

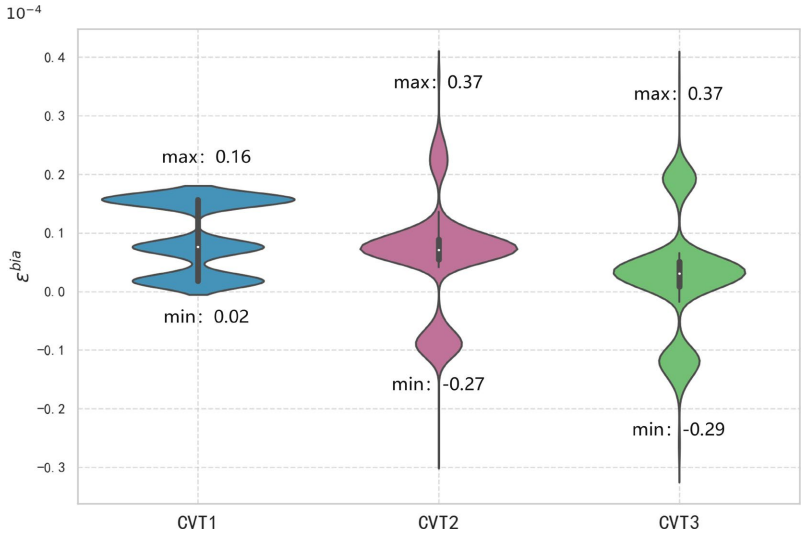

Figure 7. Violin plots of the predicted error values variation.

Table 4. Maximum absolute predicted bias values of each CVT a phase.

CVTNum-A	CVT1	CVT2	CVT3
$\left\|\varepsilon^{\text{bia}}\right\|(\%)$	0.0016	0.0037	0.0037

5.4. Effect Comparison

To evaluate the effectiveness of different monitoring methods in handling measurement errors in Capacitive Voltage Transformers, true errors of varying magnitudes were introduced into CVT1-A at different time points in the dataset. Specifically, error values of 0.002, 0.0015, and 0.0016 were added to the three sample segments, as shown in **Table 5**. Subsequently, the performance of the proposed method was compared with that of ICA based on three-phase balance [13], PCA based on three-phase balance [14].

Figure 8 shows the results of three-phase balanced independent component analysis (TP-ICA). In **Figure 8**, the statistical value in the sample interval from 0 to 1000 should not exceed the threshold, whereas in the sample interval from 1000 to 6200, the statistical value should not be lower than the threshold. However, in this interval, only 47.19% of the Q value exceeded the set threshold, resulting in failure of effective error tracking. **Figure 9** shows the results of the three-phase balanced principal component analysis (TP-PCA). Similar to the results of TP-ICA, in **Figure 9**, the threshold value was exceeded in the sample interval from 0 to 1000, whereas the statistical value was below the threshold value in the sample interval from 1000 to 6200. Similarly, in this interval, only 32.88% of the Q values exceeded the set threshold, which made it impossible to carry out effective error tracking.

Figure 10 shows the results obtained using the co-prediction matrix method. This method does not produce error changes in the 0 - 1000 sample interval, but the predicted error value in the 1000 - 2500 sample interval is consistent with 0.002 in **Table 5**. The predicted error value in the 2500 - 4000 sample interval and 4000 - 6200 sample interval were also consistent with the data in **Table 5**. This method can monitor and estimate the error amplitude in real time, which is consistent with the actual situation, and shows higher accuracy and response speed.

In summary, although TP-ICA and TP-PCA could detect anomalies to some extent, their detection rates were relatively low. The proposed method not only has high sensitivity but also effectively tracks errors in real-time, making it particularly suitable for CVT online monitoring scenarios. As shown in **Table 6**, the method developed in this study demonstrates significant advantages in handling measurement errors, efficiently identifying abnormal states without requiring complex statistical computations, providing immediate dynamic feedback on errors, and enhancing data responsiveness and overall efficiency in rapidly changing environments.

5.5. Analysis and Discussion

1) This method is suitable for recently commissioned substations. If a

Table 5. True error values set for CVT1-A in different sample segments.

Sample segment	ε^{Tru}
1000 - 2500	0.0020
2500 - 4000	0.0015
4000 - 6200	0.0016

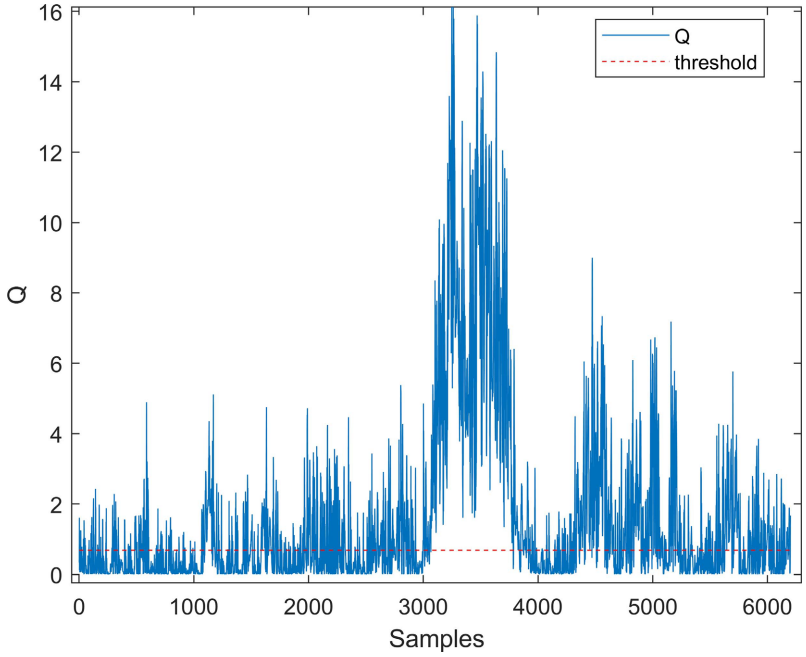

Figure 8. The performance of TP-ICA.

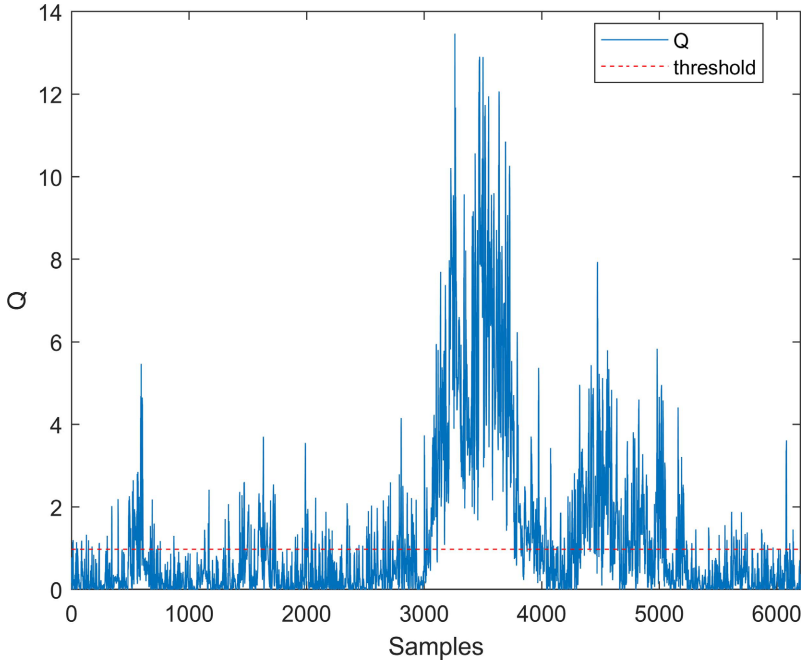

Figure 9. Performance of TP-PCA.

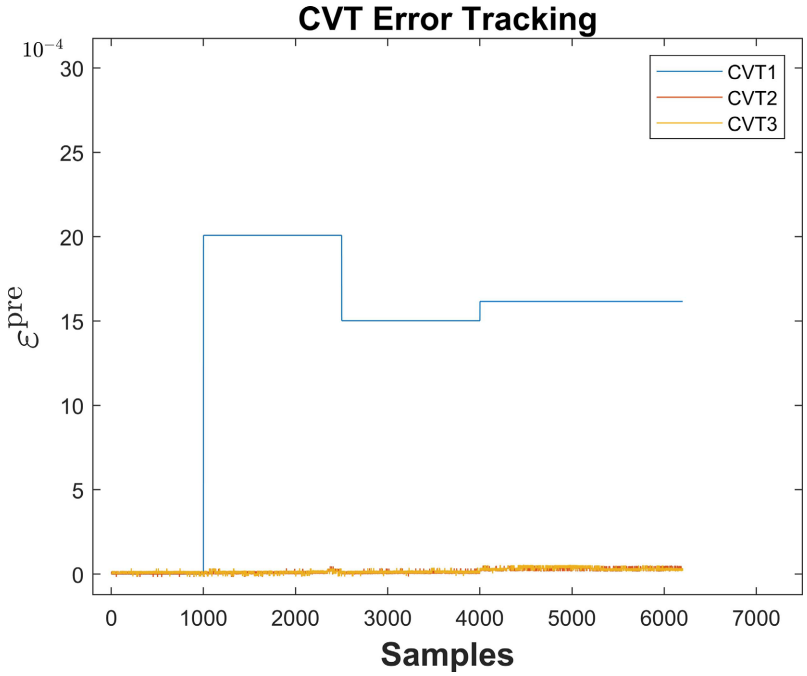

Figure 10. Performance of the co-prediction matrix method.

Table 6. Performance comparison of different monitoring methods.

Method	Anomaly portion%	Tracking error
TP-ICA	47.19%	No
TP-PCA	32.88%	No
Co-Prediction Matrix	100%	Yes

long-operating substation has recently undergone periodic on-site calibration, as long as the recent calibration error is considered as the initial error, this method can also be applied.

2) A single-phase CVT group in a station must consist of at least three or more CVTs, and the ratio error must not be changed for the same set of samples. When the group contains only two CVTs and the error of one CVT changes, Equation (13) does not hold. Therefore, it is impossible to identify faulty CVT accurately.

6. Conclusion

In this paper, an online error tracking method based on the in-phase proportional co-prediction matrix algorithm, and a fault location method are proposed. The experimental simulation results show that this method can accurately identify the CVT with error changes, and the evaluation deviation is within 0.01% for the 0.2 level CVT. Once the error beyond the set threshold is detected, the alarm can be triggered immediately and specific maintenance suggestions can be provided, so as to ensure the stable operation and safety performance of the system. In addition, compared with the traditional method, this method does not rely on the direct

measurement of the number of samples and initial values, and has higher real-time performance. This technology not only provides strong support for the preventive maintenance of power transmission and transformation facilities, but also promotes fair trading in the power market.

Conflicts of Interest

The authors declare no conflicts of interest regarding the publication of this paper.

References

[1] Chen, H., Cai, J., Li, Y., Lin, X., Chen, Z., Chen, J., *et al.* (2023) Research on the Transmission Relationship of Grid Science and Technology Innovation Indicators under the Smart Grid. 2023 2*nd International Conference on Smart Grids and Energy Systems* (*SGES*), Guangzhou, 25-27 August 2023, 19-22. https://doi.org/10.1109/sges59720.2023.10366922

[2] Omitaomu, O.A. and Niu, H. (2021) Artificial Intelligence Techniques in Smart Grid: A Survey. *Smart Cities*, **4**, 548-568. https://doi.org/10.3390/smartcities4020029

[3] Choudhary, M., Shafiq, M., Kiitam, I., Hussain, A., Palu, I. and Taklaja, P. (2022) A Review of Aging Models for Electrical Insulation in Power Cables. *Energies*, **15**, Article No. 3408. https://doi.org/10.3390/en15093408

[4] Geng, L. and Zhang, N. (2015) Simulation and Analysis on Winding Deformation of a Power Transformer in Current Transformer Connecting Manner. *Journal of Power and Energy Engineering*, **3**, 1-6. https://doi.org/10.4236/jpee.2015.34001

[5] Chen, K. and Chen, N. (2011) A New Method for Power Current Measurement Using a Coreless Hall Effect Current Transformer. *IEEE Transactions on Instrumentation and Measurement*, **60**, 158-169. https://doi.org/10.1109/tim.2010.2049234

[6] Sheng, H. and Wang, F. and Tipton IV, C. W. (2012) A Fault Detection and Protection Scheme for Three-Level DC-DC Converters Based on Monitoring Flying Capacitor Voltage. *IEEE Transactions on Power Electronics*, **27**, 685-697. https://doi.org/10.1109/tpel.2011.2161333

[7] Metwally, I. (2011) Failures, Monitoring and New Trends of Power Transformers. *IEEE Potentials*, **30**, 36-43. https://doi.org/10.1109/mpot.2011.940233

[8] Christina, A.J., Salam, M.A., Rahman, Q.M., Wen, F., Ang, S.P. and Voon, W. (2018) Causes of Transformer Failures and Diagnostic Methods—A Review. *Renewable and Sustainable Energy Reviews*, **82**, 1442-1456. https://doi.org/10.1016/j.rser.2017.05.165

[9] Moutis, P. and Alizadeh-Mousavi, O. (2021) Digital Twin of Distribution Power Transformer for Real-Time Monitoring of Medium Voltage from Low Voltage Measurements. *IEEE Transactions on Power Delivery*, **36**, 1952-1963. https://doi.org/10.1109/tpwrd.2020.3017355

[10] Singh, R.P., Sonawane, A.V., Satpute, M.S., Shirsath, D.Y. and Thakre, M.P. (2020) A Review on Traditional Methods of Condition Monitoring of Transformer. 2020 *International Conference on Electronics and Sustainable Communication Systems* (*ICESC*), Coimbatore, 2-4 July 2020, 1144-1152. https://doi.org/10.1109/icesc48915.2020.9155858

[11] Peng, Z. and Hao, L. (2021) Instrument Transformers Detection and Calibration with Synchronized Phasor Measurements. *Journal of Physics*: *Conference Series*, **1885**, Article ID: 042052. https://doi.org/10.1088/1742-6596/1885/4/042052

[12] Saponara, S., Fanucci, L., Bernardo, F. and Falciani, A. (2016) Predictive Diagnosis of High-Power Transformer Faults by Networking Vibration Measuring Nodes with Integrated Signal Processing. *IEEE Transactions on Instrumentation and Measurement*, **65**, 1749-1760. https://doi.org/10.1109/tim.2016.2552658

[13] Zhang, M., Zhang, Z. and Fan, M. (2023) Online Monitoring of Measurement Errors of CVT Based on Independent Component Analysis. In: Zeng, P.L., *et al.*, Eds., *The 37th Annual Conference on Power System and Automation in Chinese Universities* (*CUS-EPSA*), Springer Nature, 744-752. https://doi.org/10.1007/978-981-99-1439-5_68

[14] Zhang, Y., Zhang, C., Li, H., Chen, Q., Cheng, C. and Guo, P. (2022) An Online Detection Method for Capacitor Voltage Transformer Based on Load Classification. 2022 *International Conference on Sensing, Measurement & Data Analytics in the Era of Artificial Intelligence* (*ICSMD*), Harbin, 30 November-2 December 2022, 1-6. https://doi.org/10.1109/icsmd57530.2022.10058214